Preprints of the 21st IFAC World Congress (Virtual)
Berlin, Germany, July 12-17, 2020

An Interval Arithmetic Approach for Multilevel Converter Harmonic Minimization Using Parseval's Theorem

Marc Gennat * **Bernd Tibken** **

* *SWK E^2 Institute of Energy Technology and Energy Management, Hochschule Niederrhein University of Applied Science, Krefeld, Germany (e-mail: marc.gennat@hs-niederrhein.de)*
** *School of Electrical, Information and Media Engineering, University of Wuppertal, Wuppertal, Germany (e-mail: tibken@uni-wuppertal.de)*

Abstract: Multilevel converters are used for DC/AC power supply conversion, which is often applied in electric vehicle (EV) motor drives. AC conversion is done by a stepped output voltage, which provides a near-sinusoidal voltage with its fundamental frequency, but contains some higher harmonics. The elimination of several harmonics is fully implemented and well described in numerous publications, see Chiasson et al. (2003, 2004, 2005); Li et al. (2010); Tarisciotti et al. (2014), and Majed et al. (2014). In these papers the first set of undesired harmonics was eliminated, which in general was done by solving an equivalent system of equations using different methods such as resultants, Newton-Raphson (Chiasson et al. (2003)) and Optimal Minimization of Total Harmonic Distortion (OMTHD) technique, see Li et al. (2010). Higher harmonics stayed unrecognized to these optimization algorithms and delivered an undesired power spectrum to the total harmonic distortion (THD) of AC conversion.
This paper presents a novel approach to the global THD-optimization of three-phase systems taking into account all harmonics up to infinity. This global optimization is implemented using interval arithmetic, see Hansen and Walster (2003), which neither need a convex objective function nor continuous-differentiable function. Interval arithmetic computes guaranteed intervals containing the global minima. The optimum is computed with an algebraic objective function, which is derived from Parseval's theorem on a 2π periodic function.

Keywords: Harmonics elimination pulse width modulation (HEPWM), multilevel voltage source inverter (MVSI), Fourier series, Parseval's theorem, Parseval's identity, global optimization, interval arithmetic.

1. INTRODUCTION

Electric vehicles (EV) and its power supply are frequently discussed topics in the recent years. With constant growth of EV market (hybrid and battery powered) and focus on energy efficiency it is worthwhile to do further investigation on power supplies and its mathematical representation. Multilevel converters are often used as power electronics for EV power trains. Moreover, multilevel converters are broadly used in industrial applications, such as high-voltage, direct current electric power transmission (HVDC), flexible alternating current transmission system (FACTS), and static synchronous compensator (STATCOM), to name a few.

These converters switch on and off voltage once per fundamental period and per implemented H-bridge, which represents the voltage-polarity switching device. Comparing it with adjustable-speed drives (ASDs), the switching is done at significant lower frequencies (60 Hz or lower) and shows much lower voltage change rates (dV/dt). Slower switching frequencies cause less circulating currents, dielectric stresses, voltage surge, and corona discharge referring to Bell and Sung (Sept./Oct. 1997); Erdman et al. (Mar./Apr. 1996); Bonnett (Sept./Oct. 1997). This results in less motor bearing failure and motor winding insulation breakdown.

Providing a good sinusoidal voltage is the key objective. Reducing and eliminating higher harmonics, which are necessarily produced due to the switching of voltages, were investigated in Chiasson et al. (2003, 2004, 2005) and used the method of resultants from elimination theory. An eleven-level-converter with five cascaded H-bridges was investigated in Chiasson et al. (2005). Five adjustable switching angles are the degree of freedom to minimize the THD. The solution set with the smallest THD was calculated to $THD_{31} = 2.65\%$, which takes into account the distortion up to the 31^{st} harmonic.

This paper introduces a novel method to minimize THD, which provides a computable objective function summing up all undesired harmonic power components up to infinity, denoted as THD_∞. An interval arithmetic branch and bound algorithm can compute the global minimum according to Hansen and Walster (2003), even for non convex functions. This was utilized in different applications in Aschemann et al. (2005); Swiatlak et al. (2015); Gennat

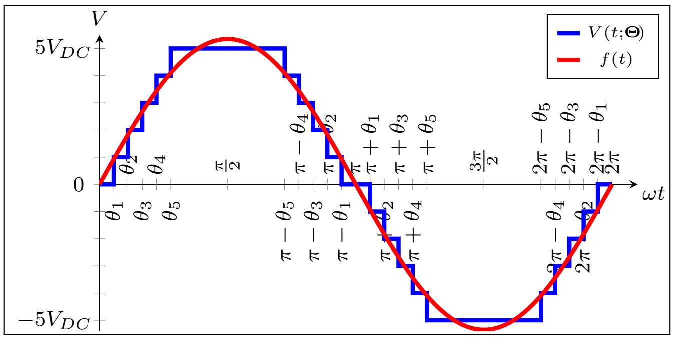

Fig. 1. Output $V(t;\vartheta)$ of an eleven-level-converter with $\theta_1 = \frac{\pi}{18}, \theta_2 = \frac{2\pi}{18}, \theta_3 = \frac{3\pi}{18}, \theta_4 = \frac{4\pi}{18}, \theta_5 = \frac{5\pi}{18}$ and the sinusoidal function $f(t)$

and Tibken (2008) and will provide in this contribution the global THD-minimum. As a result of this interval arithmetic approach THD_{31} is computed to 1.91%.

2. CASCADED SWITCHING OF MULTILEVEL INVERTER

The aim of cascaded switching is to generate a stepped output signal $V(t;\mathbf{\Theta})$, which should be "well fitted" to the desired sinusoidal signal $f(t)$. Hereby $\mathbf{\Theta} = (\theta_1\, \theta_2 \cdots \theta_s)^T$ represents the parameter set of switching angles. The parameter s defines the number of converter's H-bridges. Each θ_i denotes the switching angle respectively the time of on and off-switching of a corresponding H-bridge. Obviously, the switching angles θ_i have to lie in the first quarter of the 2π period and the condition

$$0 \le \theta_1 \le \theta_2 \le \cdots \le \theta_s \le \tfrac{\pi}{2}. \tag{1}$$

has to hold. Generally speaking, interharmonics cannot occur by multilevel converter switching. Thus, this phenomenon will not be taken into account. Further research will investigate the potential of this method to minimize THD in presence of interharmonics. The output of a stepped voltage function is shown in Fig. 1 and Fig. 2.

The overall goal of this paper is to determine the switching angles θ_i, minimizing the THD with all harmonics up to infinity. Six steps described below will lead to a computable objective function, which enables the global optimization:

- Expand $V(t;\mathbf{\Theta})$ as a Fourier series,
- define THD as desired objective function to be minimized,
- rewrite THD function in such way, that it is computable as an infinite sum of squares,
- use Parseval's theorem to compute THD as a definite integral depending on $\mathbf{\Theta}$,
- transfer the definite integral to a computable function,
- use the resulting objective function for a branch-and-bound optimization with $\mathbf{\Theta}$ as arguments.

Taking into account the switching angles θ_i of the cascaded multilevel converter, the output in $[0; \frac{\pi}{2}]$ is defined as

$$V(t;\mathbf{\Theta}) = \begin{cases} 0, \text{ if } & 0 \le t < \theta_1 \\ V_{DC}, \text{ if } & \theta_1 \le t < \theta_2 \\ 2\,V_{DC}, \text{ if } & \theta_2 \le t < \theta_3 \\ \vdots & \\ s\,V_{DC}, \text{ if } & \theta_s \le t \le \frac{\pi}{2}. \end{cases}$$

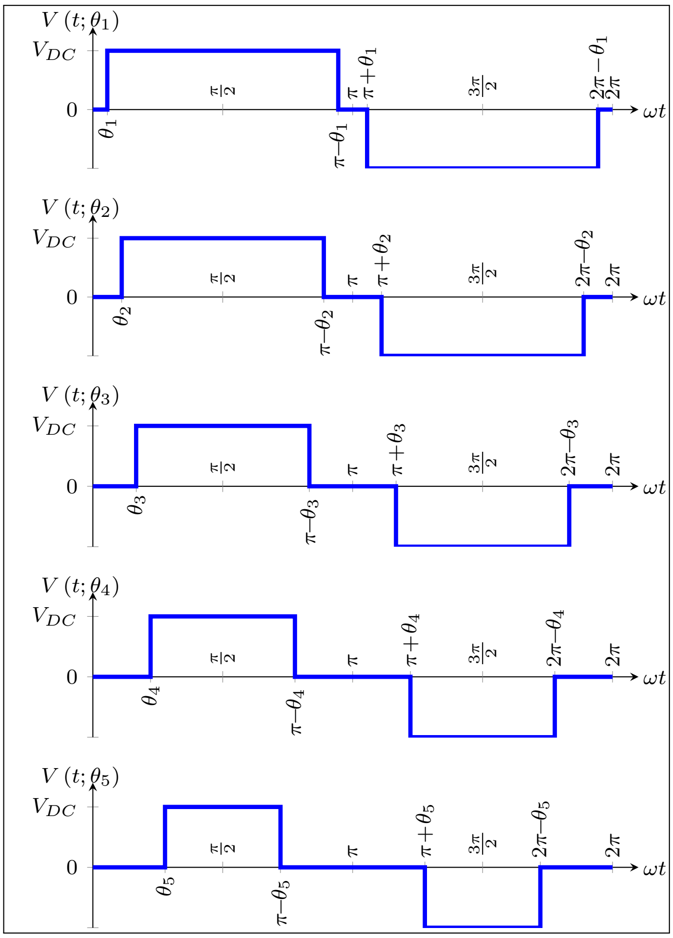

Fig. 2. Separated levels of an eleven-level-converter

To define the signal from 0 to 2π we use symmetry. This leads to $V(t;\mathbf{\Theta}) = V(\pi - t;\mathbf{\Theta})$ on $[\frac{\pi}{2}; \pi]$ and $V(t;\mathbf{\Theta}) = -V(t-\pi;\mathbf{\Theta})$ on $[\pi; 2\pi]$ (compare Fig. 1).

This 2π periodic non-sinusoidal real-valued signal $V(t;\mathbf{\Theta})$, whereby its angular frequency ω is considered as constant, can be expanded in a Fourier series, see Titchmarsh (1939); Korn and Korn (1968), with

$$V(t;\mathbf{\Theta}) = \frac{a_0}{2} + \sum_{k=1}^{\infty} \Big[a_k \cos(k\omega t) + b_k \sin(k\omega t)\Big].$$

In this paper the Fourier series is used with

$$V(t;\mathbf{\Theta}) = \sum_{k=1}^{\infty} b_k \sin(k\omega t) = \sum_{k=1}^{\infty} V_k \sin(k\omega t),$$

because the stepped waveform is symmetrical regarding the coordinate system's origin, which eliminates all a_k. The Fourier coefficients b_k represent V_k, the amplitude of the k_{th} harmonic voltage output.

The expansion of the Fourier series is shown in Chiasson et al. (2003, 2005) and can be calculated to

$$V(t;\mathbf{\Theta}) = \sum_{k=1,3,5,\cdots}^{\infty} \frac{4V_{DC}}{k\pi} \Big[\cos(k\theta_1) + \cos(k\theta_2) + \cdots + \cos(k\theta_s)\Big] sin(k\omega t).$$

The magnitudes of even harmonics are equal to zero due to the periodicity of $V(t;\mathbf{\Theta})$.

3. THD REPRESENTATION USING PARSEVAL'S THEOREM

The standard IEEE 1459-2010 in IEEE (2010) defines THD computation regarding the distorted voltage with

$$THD = \sqrt{\left(\frac{V}{V_1}\right)^2 - 1} = \sqrt{\frac{V_0^2 + \sum_{k=1}^{\infty} V_k{}^2}{V_1{}^2} - 1}. \qquad (2)$$

Direct voltage is denoted by V_0, which is zero in our case, and the first harmonic's amplitude is represented by V_1.

The tripled harmonics in a three-phase power system need not to be canceled respectively minimized in the optimization process, because they are automatically eliminated in line-to-line voltages. Hence, the above equation is computed to

$$THD = \sqrt{\frac{\sum_{k=1}^{\infty} V_k^2 - \sum_{k=1}^{\infty} V_{3k}{}^2}{V_1{}^2} - 1}.$$

All even harmonics of the voltages V_k with $k = 2, 4, 6, \cdots$ are equal to zero due to the given symmetric stepped output voltage. This facilitates the THD numerator under the square root for the given system to

$$THD_{num} = \sum_{k=1}^{\infty} V_k{}^2 - \sum_{k=1}^{\infty} V_{3k}{}^2. \qquad (3)$$

The first harmonic V_1 results from the Fourier series with

$$V_1 = \frac{4V_{DC}}{\pi} \sum_{i=1}^{s} \cos(\theta_i). \qquad (4)$$

The modulation index is defined with $m = \frac{V1}{V_{DC}}$ and can be computed from (4) with $m = \frac{4}{\pi} \sum_{i=1}^{s} \cos(\theta_i)$.

THD in (2) represents the distortion by summing up all harmonics. Using Parseval's theorem from Kelkar et al. (2002); Blagouchine and Moreau (2011) the computation can be transferred from an infinite sum to a definite integral. Starting from the integrated form of Parseval's theorem

$$\frac{1}{\pi} \int_0^{2\pi} V(t;\boldsymbol{\Theta})^2 dt = \frac{a_0{}^2}{2} + \sum_{k=1}^{\infty} \left(a_k{}^2 + b_k{}^2\right)$$

the two infinite sums in (3) can be defined with

$$\frac{1}{\pi} \int_0^{2\pi} V(t;\boldsymbol{\Theta})^2 dt = \sum_{k=1}^{\infty} V_k{}^2 \quad \text{and} \qquad (5)$$

$$\frac{1}{\pi} \int_0^{2\pi} \tilde{V}(t;\boldsymbol{\Theta})^2 dt = \sum_{k=1}^{\infty} V_{3k}{}^2, \qquad (6)$$

whereby the auxiliary function $\tilde{V}(t;\boldsymbol{\Theta})$ represents all tripled harmonics. Thus, (3) can be rewritten to

$$THD_{num} = \frac{1}{\pi} \int_0^{2\pi} V(t;\boldsymbol{\Theta})^2 - \frac{1}{\pi} \int_0^{2\pi} \tilde{V}(t;\boldsymbol{\Theta})^2. \qquad (7)$$

A main part of the novel approach of this contribution is the reformulation of V_{3k} harmonics expression in (6). This is prerequisite for the THD computation with an interval arithmetic approach.

To gain the harmonics in (7), the stepped output voltage function $\tilde{V}$ with tripled frequency has to be introduced. Starting from $V(t;\boldsymbol{\Theta})$, the tripled frequency function $\tilde{V}$ is computed with

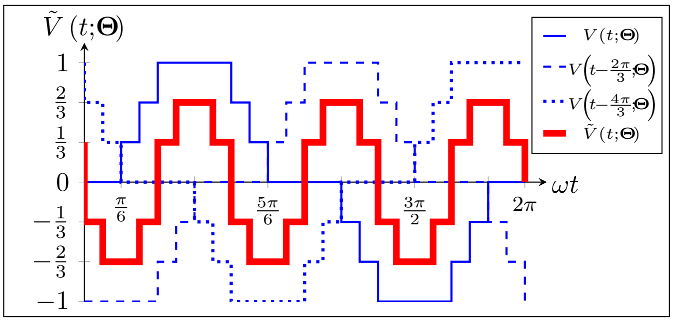

Fig. 3. Output $\tilde{V}(t;\boldsymbol{\Theta})$ with $\theta_1 = \frac{2\pi}{12}, \theta_2 = \frac{3\pi}{12}, \theta_3 = \frac{4\pi}{12}$

$$\tilde{V}(t;\boldsymbol{\Theta}) = \frac{1}{3}\left[V(t;\boldsymbol{\Theta}) + V\left(t - \frac{2\pi}{3\omega};\boldsymbol{\Theta}\right) + V\left(t - \frac{4\pi}{3\omega};\boldsymbol{\Theta}\right)\right]. \qquad (8)$$

Using trigonometric identities (8) is derived to

$$\begin{aligned} \tilde{V}(t;\boldsymbol{\Theta}) &= \frac{1}{3}\sum_{k=1}^{\infty} V_k \left\{\sin(k\omega t) + \sin\left(k\omega t - \frac{k2\pi}{3}\right) + \sin\left(k\omega t - \frac{k4\pi}{3}\right)\right\} \\ &= \frac{1}{3}\sum_{k=1}^{\infty} V_k \left\{\sin(k\omega t)\left[1 + \cos\left(\frac{k2\pi}{3}\right) + \cos\left(\frac{k4\pi}{3}\right)\right]\right. \\ &\quad \left. - \cos(k\omega t)\left[\sin\left(\frac{k2\pi}{3}\right) + \sin\left(\frac{k4\pi}{3}\right)\right]\right\}. \end{aligned}$$

For all $k \in \mathbb{N}$ the term $\sin\left(\frac{k2\pi}{3}\right) + \sin\left(\frac{k4\pi}{3}\right)$ equals to zero. With $k = 1, 4, 7, \cdots$ and $k = 2, 5, 8, \cdots$ the term $1 + \cos\left(\frac{k2\pi}{3}\right) + \cos\left(\frac{k4\pi}{3}\right)$ also equals to zero. Thus, the latter term computes to 3 with $k = 3, 6, 9, \cdots$ and $\tilde{V}$ results in

$$\tilde{V}(t;\boldsymbol{\Theta}) = \sum_{k=1}^{\infty} V_{3k} \sin(3k\omega t). \qquad (9)$$

According to this, the sum of squares of all tripled harmonics equals to the above introduced equation (6). Hence, the terms in (3), (4), (5), (6), and (9) are used to compute the THD (2) to

$$THD = \sqrt{\frac{\frac{1}{\pi}\int\limits_0^{2\pi} V(t;\boldsymbol{\Theta})^2 dt - \frac{1}{\pi}\int\limits_0^{2\pi} \tilde{V}(t;\boldsymbol{\Theta})^2 dt}{\left(\frac{4V_{DC}}{\pi}\sum\limits_{i=1}^{s}\cos(\theta_i)\right)^2} - 1}. \qquad (10)$$

4. COMPUTING AN OBJECTIVE FUNCTION

The objective function derives from THD computation of (10). Omitting the square root does not affect the optimum parameter set. Consequently, the objective is defined with

$$\begin{aligned} J &= \frac{THD_{num}}{\left(\frac{4V_{DC}}{\pi}\sum\limits_{i=1}^{s}\cos(\theta_i)\right)^2} \\ &= \frac{\int\limits_0^{2\pi} V(t;\boldsymbol{\Theta})^2 dt - \int\limits_0^{2\pi} \tilde{V}(t;\boldsymbol{\Theta})^2 dt}{\frac{16V_{DC}{}^2}{\pi}\left(\sum\limits_{i=1}^{s}\cos(\theta_i)\right)^2}. \end{aligned} \qquad (11)$$

The computation of (11) needs further processing of $\tilde{V}(t;\boldsymbol{\Theta})^2$, which is compound by three phase-shifted $V(t;\boldsymbol{\Theta})$ functions. For notation reasons $W(\alpha) = V(t - \alpha;\boldsymbol{\Theta})$ is used to rewrite V with

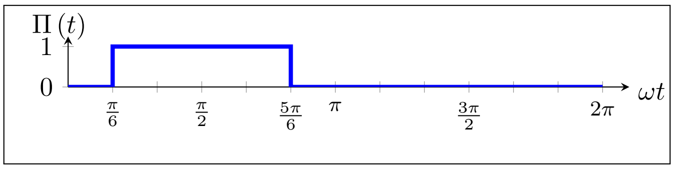

Fig. 4. Rectangular function $\Pi\left(\frac{t-\pi/2}{\pi-\pi/3}\right)$

$$\tilde{V}(t;\boldsymbol{\Theta})^2 = \left(\frac{1}{3}\left[W(0) + W\left(\tfrac{2\pi}{3}\right) + W\left(\tfrac{4\pi}{3}\right)\right]\right)^2.$$

The introduction of $\tau = \frac{2\pi}{3}$ and $\upsilon = \frac{4\pi}{3}$ rewrites $\tilde{V}^2$ to

$$\begin{aligned}\tilde{V}^2(t;\boldsymbol{\Theta}) = \frac{1}{9}\Big[&W(0)^2 + 2W(0)\, W\left(\tfrac{2\pi}{3}\right) + \\ &W(\tau)^2 + 2W(\tau)\, W\left(\tau + \tfrac{2\pi}{3}\right) + \\ &W(\upsilon)^2 + 2W(\upsilon)\, W\left(\upsilon + \tfrac{2\pi}{3}\right)\Big].\end{aligned}$$

Using above shown 120° phase shifts, $\bar{W}$ is introduced with

$$\begin{aligned}\bar{W}(t) &= W(0)^2 + 2W(0)\quad W\left(\tfrac{2\pi}{3}\right)\\ &= V(t;\boldsymbol{\Theta})^2 + 2V(t;\boldsymbol{\Theta})\quad V\left(t-\tfrac{2\pi}{3};\boldsymbol{\Theta}\right),\end{aligned}$$

and $\tilde{V}^2$ can be edited to

$$\tilde{V}(t;\boldsymbol{\Theta})^2 = \frac{1}{9}[\bar{W}(t) + \bar{W}(t+\tau) + \bar{W}(t+\upsilon)]. \tag{12}$$

To compute THD_{num} in (7), Parseval's theorem expression from (6) can be used with (12) and with $\tau_i(t) = \frac{2i\pi}{3}$ as

$$\frac{1}{\pi}\int_0^{2\pi} \tilde{V}(t;\boldsymbol{\Theta})^2 dt = \frac{1}{9\pi}\int_0^{2\pi}\sum_{i=0}^{2} \bar{W}(\tau_i + t)dt = \frac{1}{3\pi}\int_0^{2\pi}\bar{W}(t)dt.$$

The latter equation holds, because the integration of three 120° phase shifted periodical functions computes the same result three times. Using this representation of the integrated $\tilde{V}^2$, the THD numerator under the square root in (3) is expressed by

$$THD_{num} = \frac{1}{\pi}\int_0^{2\pi} V(t;\boldsymbol{\Theta})^2 dt - \frac{1}{3\pi}\int_0^{2\pi}\bar{W}(t)\, dt. \tag{13}$$

At this point, the voltage switching must be modeled. This starts with the rectangular function

$$\Pi(t) = \mathrm{rect}(t) = \begin{cases} 1, & \text{if } |t| < \frac{1}{2}, \frac{1}{2}, \text{ if } |t| = \frac{1}{2}, \\ 0, & \text{otherwise}\end{cases}$$

and leads to the rewritten stepped output voltage function $V(t;\boldsymbol{\Theta})$ with

$$V(t;\boldsymbol{\Theta}) = V_{DC}\sum_{i=1}^{s}\left[\Pi\left(\frac{t-\frac{\pi}{2}}{\pi - 2\theta_i}\right) - \Pi\left(\frac{t-\frac{3\pi}{2}}{\pi-2\theta_i}\right)\right].$$

The output of $V(t;\boldsymbol{\Theta})$ is already shown in Fig. 1. The 2π periodicity of $V(t;\boldsymbol{\Theta})$ and the sum of s rectangular functions $\Pi(t)$ have to be taken into account. For this reason, $r(t;m,\boldsymbol{\Theta})$ and its abbreviation $R(m)$ as the sum over all rectangular functions of the referring switching angles θ_1 to θ_s, its midpoint parameter m, and $\mathbb{Z} = \{-\mathbb{N}, 0, \mathbb{N}\}$ is defined with

$$R(m) = r(t;m,\boldsymbol{\Theta}) = \sum_{k\in\mathbb{Z}}\sum_{i=1}^{s}\Pi\left(\frac{t-m+2k\pi}{\pi-2\theta_i}\right) \tag{14}$$

Using (14) the computation of $V(t;\boldsymbol{\Theta})^2$ results in

$$V(t;\boldsymbol{\Theta})^2 = {V_{DC}}^2\left[R\left(\tfrac{\pi}{2}\right)^2 - 2R\left(\tfrac{\pi}{2}\right) R\left(\tfrac{3\pi}{2}\right) + R\left(\tfrac{3\pi}{2}\right)^2\right]. \tag{15}$$

The first summand in (13) is easy to compute by integrating the rectangular functions on the right hand side of (15), because there are no overlapping rectangles due to the angle conditions (1). Thus, the first summand of THD's numerator (13) is transferred to

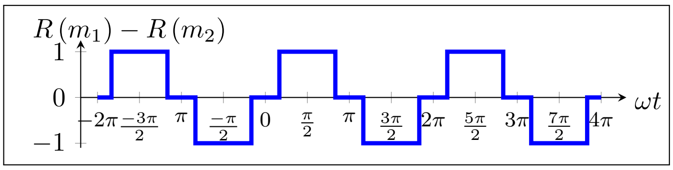

Fig. 5. Rectangular function $R\left(\frac{\pi}{2}\right) - R\left(\frac{3\pi}{2}\right)$ with $\theta = \frac{\pi}{6}$

$$\frac{1}{\pi}\int_0^{2\pi} V(t;\boldsymbol{\Theta})^2 dt = \frac{2{V_{DC}}^2}{\pi}\sum_{i=1}^{s}(2i-1)(\pi - 2\theta_i). \tag{16}$$

To compute the second summand of (13) some additional calculations have to be done, which leads to

$$\begin{aligned}2V(t;\boldsymbol{\Theta})\, V\left(t-\tfrac{2\pi}{3};\boldsymbol{\Theta}\right) = 2{V_{DC}}^2\Big[&R\left(\tfrac{\pi}{2}\right) R\left(\tfrac{-\pi}{6}\right)\\ -R\left(\tfrac{\pi}{2}\right) R\left(\tfrac{5\pi}{6}\right) - R\left(\tfrac{3\pi}{2}\right) R\left(\tfrac{-\pi}{6}\right) + &R\left(\tfrac{3\pi}{2}\right) R\left(\tfrac{5\pi}{6}\right)\Big],\end{aligned}$$

whereby the output of $R(m_1)\cdot R(m_2)$ is shown in Fig. 6. The function $2V(t;\boldsymbol{\Theta})V\left(t-\frac{2\pi}{3};\boldsymbol{\Theta}\right)$ is π periodical, and the maximum width of rectangles is π due to the initial angle conditions. Accordingly, the integral of $2V(t;\boldsymbol{\Theta})\, V\left(t-\frac{2\pi}{3}\right)$ from 0 to π equals with the integral from π to 2π. For reasons of simplification this results in an auxiliary function $h(\boldsymbol{\Theta})$ defined with

$$\begin{aligned}h(\boldsymbol{\Theta}) &= \int_0^{2\pi} 2V(t;\boldsymbol{\Theta})\, V\left(t-\tfrac{2\pi}{3};\boldsymbol{\Theta}\right) dt\\ &= 2{V_{DC}}^2\int_0^{\pi} R\left(\tfrac{\pi}{2}\right) R\left(\tfrac{-\pi}{6}\right) - R\left(\tfrac{\pi}{2}\right) R\left(\tfrac{5\pi}{6}\right) dt\\ &= 2{V_{DC}}^2\sum_{i=1}^{s}\sum_{k=1}^{s}\min\left(\max\left(\theta_i + \theta_k, \tfrac{\pi}{3}\right), \tfrac{2\pi}{3}\right) - \tfrac{2\pi}{3}.\end{aligned} \tag{17}$$

The function `max(a,b)` returns the higher value of a or b, respectively `min(a,b)` returns the lower value. To clarify the dependency of $h(\boldsymbol{\Theta})$ from switching angles θ_i, the graph of the piecewise differentiable function (17) with one switching angle θ_1 is shown in Fig. 7.

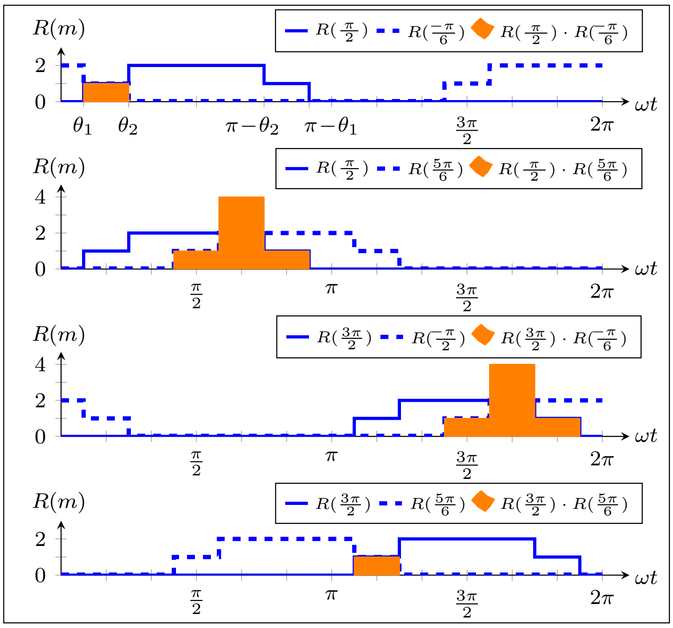

Fig. 6. Plots of $R(m_1)\cdot R(m_2)$ with $\boldsymbol{\Theta} = (\theta_1\ \theta_2)^T = \left(\frac{\pi}{12}\ \frac{3\pi}{12}\right)^T$

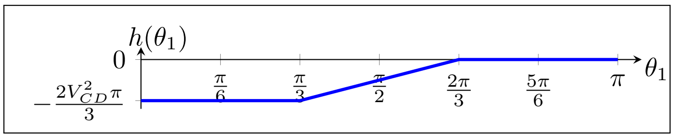

Fig. 7. Plot of function $h(\mathbf{\Theta})$ with one switching angle θ_1

Finally, using the auxiliary function (17) the second summand (13) of THD numerator under the square root (7) is denoted with

$$\frac{1}{3\pi}\int_0^{2\pi}\bar{W}(t)dt = \frac{2{V_{DC}}^2}{3\pi}\sum_{i=1}^{s}\Bigg\{(2i-1)(\pi-2\theta_i)$$
$$+2\sum_{k=1}^{s}\left[\min\left(\max\left(\theta_i+\theta_k,\tfrac{\pi}{3}\right),\tfrac{2\pi}{3}\right)-\tfrac{2\pi}{3}\right]\Bigg\}, \qquad (18)$$

and all elements of the objective (11) are computable. The objective function can now be noted by applying the right hand sides of (4), (16), and (18) with

$$J = \frac{\pi}{12\left[\sum_{i=1}^{s}\cos(\theta_i)\right]^2}\sum_{i=1}^{s}\Bigg[(2i-1)(\pi-2\theta_i)-$$
$$\sum_{k=1}^{s}\left[\min\left(\max\left(\theta_i+\theta_k,\tfrac{\pi}{3}\right),\tfrac{2\pi}{3}\right)-\tfrac{2\pi}{3}\right]\Bigg]. \qquad (19)$$

This objective function (19) takes into account all THD's harmonics up to infinity, and this representation is computable with common computer systems. An output of J is shown in Fig. 8, using two switching angles. The resulting THD is calculated with

$$THD_\infty = \sqrt{J-1} \qquad (20)$$

5. INTERVAL ARITHMETIC APPROACH RESULTS

In Chiasson et al. (2003, 2005) the THD is computed with

$$THD_{31} = \sqrt{\frac{V_5^2+V_7^2+V_{11}^2+V_{13}^2+V_{17}^2+\cdots+V_{31}^2}{{V_1}^2}}.$$

This THD computation stops the distorted harmonic summation at the 31st harmonic. There is no explanation for stopping at 31st in the referenced publications. Due to filtering of higher frequencies in real-world applications, this THD_{31} computation could be sufficient.

A standard interval arithmetic branch and bound-algorithm, which provides a guaranteed global minimum, is shown in Hansen and Walster (2003). A constraint optimization algorithm was applied on the objective function (19) using this interval arithmetic approach of Hansen. The global minimum was computed with Matlab, see The MathWorks (2018), and `INTLAB`-toolbox from Rump (1999). It took over 5.4 million iterations to satisfy the termination criteria of THD^*'s lower and upper bound distance, which was set to 10^{-11}. The algorithm returns intervals of regions containing the optimal parameter set switching angles. The best found parameter set θ^* is given in Tab. 1. The modulation index was not scope of this computation. In further research this could be taken into account by introducing additional constraints.

This parameter set provides the minimal $THD_\infty = 3.88\%$ and $THD_{31} = 1.91\%$, rounded on three digits. The latter was computed for comparison reasons with the results from Chiasson et al. (2005), where the optimal THD was

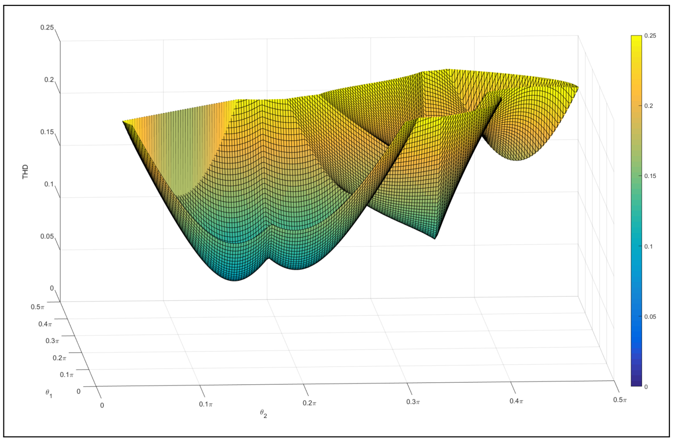

Fig. 8. *THD* plot with two parameters θ_1 and θ_2

given by $THD_{31} = 2.65\%$. Using the referring switching angles parameter set θ, the computation of (2) leads to $THD_\infty = 12.1\%$. The resulting switching angles are also noted in Tab. 1.

	THD_∞^* / THD_{31}^* / **modulation**	$\theta^* \Big/ \frac{\mathbf{2\pi}}{\mathbf{360°}}$
Global optimization of objective function (19) using interval arithmetic approach	3.8764837%	3.2459166°
	1.9099464%	9.7797646°
	$m = 4.617$	16.445426°
		26.933938°
		38.522666°
Best solution given in Chiasson et al. (2003, 2005) with constraints $V_{5,7,11,13} = 0$	12.062863%	9.3005193°
	2.6480947%	34.407215°
	$m = 3.203$	42.069638°
		59.906517°
		81.554343°

Table 1. Optimization Results

6. CONCLUSIONS

In this paper an interval arithmetic approach was applied to a novel objective function formulation, which computes the THD of multilevel converters. The objective reformulation utilizes Parseval's theorem to sum up all harmonics up to infinity. The here introduced reformulation of THD_∞ computation was not found by the authors in literature for three-phase multilevel converters.

Chiasson et al. (2003, 2004, 2005) eliminate the fifth, seventh, eleventh, and 13th harmonic to minimize THD. In the referenced papers THD computation stops at the 31st. The results of Chiasson et. al. and the interval arithmetic approach are compared in 1. THD_{31} distortion is improved from 2.65% down to 1.91%, which is a reduction of about a third. Moreover, the interval arithmetic approach improves THD_∞ from 12.1% down to 3.88%. Some real-world applications, which filter high frequencies, would not suffer from high THD_∞. In this case THD_{31} is a good objective. Applications without filtering high frequencies would benefit from this novel THD_∞ formulation and optimization approach.

The recomputed normalized harmonics from Chiasson et al. (2005) are shown in Fig. 9. Here, as desired, the fifth, seventh, eleventh, and 13th disappear. The remaining non-tripled and odd harmonics sum up to the THD.

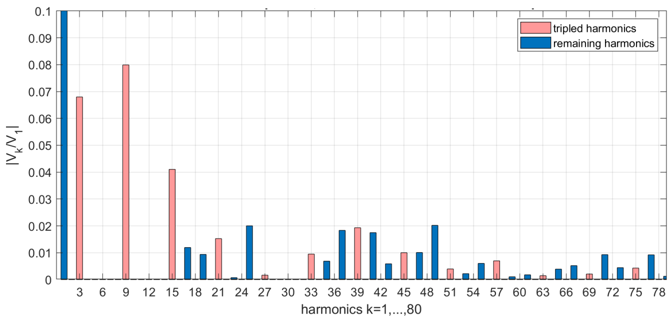

Fig. 9. Normalized harmonics, recomputed using results from Chiasson et al. (2005)

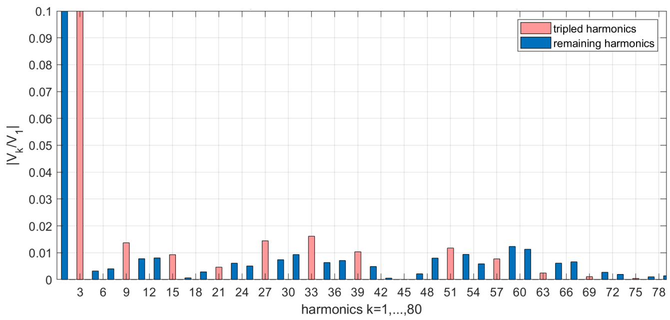

Fig. 10. Normalized harmonics derived from (19) global optimization

Especially the 25^{th} contribute some distortion to THD_{31}. The normalized harmonics computed with the here introduced novel method of THD-minimization are presented in Fig. 10. The optimization algorithm does not eliminate any harmonic. It minimizes the infinite sum of all non-tripled and odd harmonics. Even with harmonic values in the lower frequency domain the THD_{31} and THD_{∞} was improved using this interval arithmetic approach.

In future work n-level-converters and its optimal THD computation could be investigated. Moreover, interharmonics could be researched. Today it is not clear, if an interval arithmetic approach could provide significant improvement.

REFERENCES

Aschemann, H., Rauh, A., Kletting, M., Hofer, E., Gennat, M., and Tibken, B. (2005). Interval analysis and nonlinear control of wastewater plants with parameter uncertainty. *IFAC Proceedings Volumes*, 38(1), 55–60.

Bell, S. and Sung, J. (Sept./Oct. 1997). Will your motor insulation survive a new adjustable frequency drive? *IEEE Transactions on Industry Applications*, 33, 1307–1311.

Blagouchine, C.V. and Moreau, E. (2011). Analytic method for the computation of the total harmonic distortion by the cauchy method of residues. *IEEE Transactions on Communications*, 59(9), 2478–2491.

Bonnett, A.H. (Sept./Oct. 1997). A comparison between insulation systems available for pwm-inverter-fed motors. *IEEE Transactions on Industry Applications*, 33, 1331–1341.

Chiasson, J., Tolbert, L., McKenzie, K., and Du, Z. (2003). Elimination of harmonics in a multilevel converter using the theory of symmetric polynomials and resultants. In *Proc. IEEE Conference on Decision and Control*, 3507–3512. Hawaii, USA.

Chiasson, J., Tolbert, L., McKenzie, K., and Du, Z. (2004). A complete solution to the harmonic elimination problem. *IEEE Transactions on Power Electronics*, 19, 491 – 499.

Chiasson, J., Tolbert, L., McKenzie, K., and Du, Z. (2005). Elimination of harmonics in a multilevel converter using the theory of symmetric polynomials and resultants. *IEEE Transactions on Control Systems Technology*, 13(2), 216–223.

Erdman, J., Kerkman, R., Schlegel, D., and Skibinski, G. (Mar./Apr. 1996). Effect of pwm inverters on ac motor bearing currents and shaft voltages. *IEEE Transactions on Industry Applications*, 32, 250–259.

Gennat, M. and Tibken, B. (2008). Computing guaranteed bounds for uncertain cooperative and monotone nonlinear systems. *IFAC Proceedings Volumes*, 41(2), 4846–4851.

Hansen, E. and Walster, G.W. (2003). *Global optimization using interval analysis: revised and expanded*, volume 264. CRC Press.

IEEE (2010). Ieee standard definitions for the measurement of electric power quantities under sinusoidal, nonsinusoidal, balanced, or unbalanced conditions no. 1459. URL `https://standards.ieee.org/findstds/standard/1459-2010.html`.

Kelkar, S.S., Grigsby, L.L., and Langsner, J. (2002). An extension of parseval's theorem and its use in calculating transient energy in the frequency domain. *IEEE Transactions on Industrial Electronics*, IE-30, 42–45.

Korn, G.A. and Korn, T.M. (1968). *Mathematical Handbook for Scientists and Engineers. Definitions, Theorems, and Formulas for Reference and Review.* McGraw–Hill, New York.

Li, Q., He, Z., and Tang, G. (2010). Investigation of the harmonic optimization approaches in the new modular multilevel converters. In *Proc. Power and Energy Engineering Conference (APPEEC)*. Chengdu, China.

Majed, A., Salam, Z., and Amjad, A.M. (2014). Hepwm implementation for fifteen level cascaded inverter using field programmable gate array. In *Proc. IEEE Conference on Energy Conversion (CENCON)*, 331–335. Johor Bahru, Malaysia.

Rump, S. (1999). INTLAB - INTerval LABoratory. In T. Csendes (ed.), *Developments in Reliable Computing*, 77–104. Kluwer Academic Publishers, Dordrecht.

Swiatlak, R., Tibken, B., Paradowski, T., and Dehnert, R. (2015). An interval arithmetic approach for the estimation of the robust domain of attraction for nonlinear autonomous systems with nonlinear uncertainties. In *2015 American Control Conference (ACC)*, 2679–2684. IEEE.

Tarisciotti, L., Zanchetta, P., Watson, A., Bifaretti, S., Clare, J., and Wheeler, P. (2014). Active dc voltage balancing pwm technique for high-power cascaded multilevel converters. *IEEE Transactions on Industrial Electronics*, 61(11), 6157–6167.

The MathWorks (2018). Matlab and optimization toolbox release 2018a. URL `https://www.mathworks.com/products/matlab.html`.

Titchmarsh, E.C. (1939). *The Theory of Functions*. Oxford University Press, Oxford, 2nd edition edition.